fortune Journals

Research Article

JOURNAL OF SURGERY AND RESEARCH

ISSN: 2640-1002

Locally Administered Photothermal Therapy for Breast Cancer using Endolysosome-Targeted Indocyanine Green Conjugated with Polycation

Saori Fujiwara[1,2†], Toru Yoshitomi[1,†*], Aoi Hoshi[2], Van Thi Hong Doan[1], Yoshiki Komatsu[1,2,5], Huajian Chen[1], Naoki Kawazoe[1], Guoping Chen[1], Azusa Terasaki[3], Hiroko Bando[4], Hisato Hara[4], and Hirofumi Matsui[5*]

Abstract

Near-infrared photothermal therapy using indocyanine green has a great potential of anti-tumor therapy against deep tumor tissue owing to its biological transparency window and high spatiotemporal selectivity. However, even intratumor administration of indocyanine green does not show high antitumor efficacy. To improve the anti-tumor efficacy of indocyanine green, in this study, we have developed a locally administered photothermal therapy using indocyanine green with polycations bearing quaternary ammonium salt groups, referred to as aICG. The aICG was accumulated in endolysosome *via* endocytosis after cell adhesion by electrostatic interaction, and induced apoptosis by laser irradiation at 808 nm, while low-molecular-weight ICG distributed in the cytoplasm. Photothermal therapy with intratumor injection of aICG showed a higher anti-tumor effect upon the light irradiation at 808 nm, compared to low-molecular-weight ICG. In addition, the treatment with aICG did not cause any adverse effects such as weight loss, and hepatic and renal dysfunctions. Therefore, aICG has a potential as photothermal agent for locally administered photothermal therapy.

Keywords: Endolysosome; Polycation; Indocyanine green; Photothermal therapy

Introduction

Globally, the number of new cancer patients increased from 18.7 million in 2010 to 23.6 million in 2019, which was an increase of 26.3%. Similarly, the number of deaths from cancer increased by 20.9% from 8.29 million in 2010 to 10.0 million in 2019 [1]. Among female population, breast cancer with the highest incidence is the leading cause of death from all cancer [2]. Currently, for patients who can undergo surgery, preoperative chemotherapy is a standard treatment to reduce the size of the tumor. Successful preoperative chemotherapy allows breast-conserving therapy [3]. However, patients with advanced age or underlying diseases such as cardiac, respiratory, and renal diseases cannot receive chemotherapy due to severe side effects. Therefore, to develop noninvasive local treatment is desired as an alternative to chemotherapy. In addition, noninvasive local treatment is also important for advanced recurrent breast cancer patients for whom surgery is not indicated, as it improves the quality of life for the patients.

So far, near-infrared (NIR)-photothermal therapy (PTT) has been widely studied as a noninvasive local treatment against breast cancers owing to its biological transparency window and high spatiotemporal selectivity [4-7].

Affiliation:

[†]Equal contribution: S.F. and T.Y. contributed equally to this work.

[1]Research Center for Macromolecules and Biomaterials, National Institute for Materials Science, 1-1 Namiki, Tsukuba, Ibaraki 305-0044, Japan

[2]Graduate School of Comprehensive Human Sciences, University of Tsukuba, 1-1-1 Tennodai, Tsukuba, Ibaraki 305-8577, Japan

[3]Department of Breast-Thyroid-Endocrine Surgery, University of Tsukuba Hospital, 2-1-1 Amakubo, Tsukuba, Ibaraki 305-8576, Japan

[4]Division of Breast and Endocrine Surgery, Faculty of Medicine, University of Tsukuba, 1-1-1 Tennodai, Ibaraki 305-8575, Japan

[5]Division of Gastroenterology, Faculty of Medicine, University of Tsukuba, 1-1-1 Tennodai, Ibaraki 305-8575, Japan

***Corresponding author:**
Toru Yoshitomi, Research Center for Macromolecules and Biomaterials, National Institute for Materials Science, 1-1 Namiki, Tsukuba, Ibaraki 305-0044, Japan

Hirofumi Matsui, Division of Gastroenterology, Faculty of Medicine, University of Tsukuba, 1-1-1 Tennodai, Ibaraki 305-8575, Japan

Citation: Saori Fujiwara, Toru Yoshitomi, Aoi Hoshi, Van Thi Hong Doan, Yoshiki Komatsu, Huajian Chen, Naoki Kawazoe, Guoping Chen, Azusa Terasaki, Hiroko Bando, Hisato Hara, and Hirofumi Matsui. Locally administered photothermal therapy for breast cancer using endolysosome-targeted indocyanine green conjugated with polycation. Journal of Surgery and Research. 7 (2024): 122-133.

Received: February 15, 2024
Accepted: February 23, 2024
Published: March 14, 2024

Fujiwara S., J Surg Res 2024
DOI:10.26502/jsr.10020350

NIR-PTT uses photothermal agents and irradiation with NIR light [8]. By the NIR light irradiation, photothermal agents convert photon energy into heat and release heat locally to directly kill cancer cells. Indocyanine green (ICG) is widely used for identification of sentinel nodes during breast cancer surgery and liver function tests in clinical practice [9, 10]. In recent years, the NIR photothermal effect of ICG has widely attracted much attention [11]. However, its effectiveness is not sufficient and even intratumor administration of ICG does not show high antitumor efficacy. We hypothesized that one of the reasons for the lower effect of ICG is its poor intracellular targeting property due to diffusion into cells. Here, we focused on lysosomes which are the main digestive organelles. The function of lysosomes is to maintain the cellular homeostasis by degradation and recycling of cellular waste using digestive enzymes [12]. Yet, a release of digestive enzymes in lysosomes by lysosomal membrane permeabilization or lysosomal rupture become lethal threat to cellular integrity, leading to apoptosis [13-15]. Therefore, lysosomes are emerging as attractive targets for anticancer therapy with PTT.

Recently, we developed locally administered photodynamic therapy for the treatment of gastrointestinal cancers using photosensitizer porphyrin with polycations consisting of quaternary ammonium salt groups [16]. Conjugation of polycation consisting of quaternary ammonium salt groups with porphyrin leads to an accumulation in the lysosome, because polycation bearing quaternary ammonium salt groups adhere to cell membranes through electrostatic interactions and are uptaken in endosome in the cells *via* endocytosis. Then, endosome is fused with lysosome to be endolysosome [16]. Interestingly, the light irradiation with a 635 nm laser after its accumulation in lysosomes improves apoptotic activity [16]. However, as breast cancer requires a treatment of deep tumor tissue than gastrointestinal cancers, the NIR-PTT is suitable. To improve the performance of NIR-sensitive ICG, in this study, we developed ICG conjugated with polycations bearing quaternary ammonium salt groups, which is referred to as adhesive ICG (aICG). In this study, the anti-tumor efficacy of locally administered PTT using aICG as a photothermal agent was investigated.

Materials and Methods

Intracellular localization

Synthesis of aICG is described in supporting information. 4T1 cell line, which is breast carcinoma of BALB/c mouse, was purchased from Riken Cell Bank (Tsukuba, Japan). The cells were seeded on glass bottom dish at density of 5.0×10^3 cells per glass area of glass bottom dish and incubated for 2 d inside a 5% CO_2 incubator. The culture medium was replaced to 180 µL of RPMI without phenol red and fetal bovine serum (FBS). Twenty microliters of ICG or aICG solution was added at the final ICG concentration of 1.3 µM, followed by the incubation for 1 d inside the 5% CO_2 incubator. The lysosome in the cells was stained by Lysotracker Green DND-26 (Invitrogen, CA, USA), followed by staining with Hoechst 33258 (Dojin Chemical, Kumamoto, Japan) after fixation with 4% paraformaldehyde. The cells were observed using a STELLARIS 8 confocal microscope (Leica Microsystems, Wetzlar, Germany).

Cellular uptake

4T1 cells were seeded in the each well of 24-well plates at 2.5×10^4 cells per well and incubated at 37 °C inside the 5% CO_2 incubator for 2 d. After the medium was removed, 400 µL of fresh medium without FBS/phenol red containing ICG or aICG was added at the final ICG concentration of 1.3 µM, and the cells were incubated inside the 5% CO_2 incubator for 24 h. Then, the cells were washed with PBS three times, and harvested using trypsin-EDTA. The number of cells was counted using a hemocytometer. RIPA buffer (100 µL) was added to the cell suspension with same cellular density. The fluorescence spectra of ICG and aICG in cell lysates were measured using a fluorescent spectrometer (JASCO FP-8500, Jasco, Tokyo, Japan). The excitation wavelength was 760 nm. The emission wavelength was 790-850 nm.

Cell viability assay

4T1 cells were seeded on 96-well microplate at density of 5.0×10^3 cells per well and incubated inside the 5% CO_2 incubator for 1 d. The culture medium was replaced to 90 µL of RPMI without phenol red and FBS, followed by addition of 10 µL of ICG or aICG solution at the final ICG concentration of 1.3 µM. The cells were incubated inside the 5% CO_2 incubator for 1 d. The cells were irradiated with 808 nm light at 0.9 W/cm^2 for 15 min (810 J/cm^2) at room temperature using a semiconductor laser (CivilLaser, Hangzhou, China), and incubated for 1 d. The temperature of the culture medium during irradiation was recorded using a thermal camera (FLIR C5, FLIR Systems, France). After ten microliters of WST-1 was added, the cells were incubated for 2 h, followed by measurement of the absorbance using a Benchmark Plus microplate spectrophotometer (Bio-Rad, Hercules, USA) at 440 nm. In addition, the cells were stained with a LIVE/DEAD cell staining kit containing propidium iodide (PI) and calcein-AM, followed by microscopic observation with a fluorescence microscope (BZ-710; Keyence, Osaka, Japan).

Intracellular ROS generation

4T1 cells were seeded on 24-well microplate at density of 5.0×10^4 cells per well and incubated inside 5% CO_2 incubator at 37 °C for 1 d. The culture medium was replaced to 450 µL of RPMI without phenol red and FBS. Fifty microliters of ICG or aICG solution at the concentration of 13 µM was added, followed by the incubation for 1 d. DCFH-DA was added at the final concentration of 0.1 µM, followed by the further incubation for 15 min. The cells were washed three

Citation: Saori Fujiwara, Toru Yoshitomi, Aoi Hoshi, Van Thi Hong Doan, Yoshiki Komatsu, Huajian Chen, Naoki Kawazoe, Guoping Chen, Azusa Terasaki, Hiroko Bando, Hisato Hara, and Hirofumi Matsui. Locally administered photothermal therapy for breast cancer using endolysosome-targeted indocyanine green conjugated with polycation. Journal of Surgery and Research. 7 (2024): 122-133.

Fujiwara S., J Surg Res 2024
DOI:10.26502/jsr.10020350

times with PBS to remove extracellular DCFH-DA, then 500 µL of PBS was added in each well. The cells were irradiated with 808 nm laser at 0.9 W/cm^2 for 15 min (810 J/cm^2) at room temperature. After the cells were harvested with trypsin/EDTA treatment, the fluorescence intensity in the cells was quantified using a BD Accuri™™ C6 flow cytometer (BD Biosciences San Jose, CA, USA).

Apoptosis/Necrosis assay

4T1 cells were seeded on 24-well microplate at density of 5.0 × 10^4 cells per well and incubated for 2 d. The culture medium was replaced to 360 µL of RPMI without phenol red and FBS. Forty microliters of ICG or aICG solution were added, followed by the incubation. The cells were irradiated with 808 nm laser at 0.9 W/cm^2 for 15 min (810 J/cm^2) at room temperature. The culture medium was replaced to 500 µL of RPMI. The cells were incubated for 0.5 and 3 h. Apoptosis and necrosis of the cells were detected using the Apoptosis/Necrosis assay kit, and observed using a fluorescence microscope.

Animals

Female BALB/c mice (5-6 weeks old) were purchased from CREA Japan Inc. (Tokyo, Japan). Five animals was housed per cage and provided water and mouse chow ad libitum. The animals were maintained in a standard 12 h light-dark cycle. Animal experiments were approved by the Laboratory Animal Research Center of the University of Tsukuba (approval number No. 22-078).

In vivo anti-cancer NIR-PTT by local administered aICG

Female BALB/c mice (5-6 weeks old) were used for preparing tumor-bearing mice. After shaving the back of the mice, 5.0 × 10^5 luciferase-expressing 4T1 cells (4T1-Luc, Riken Cell Bank, Tsukuba, Japan) were subcutaneously injected in the right side of the back. When the tumor volume reached 30-50 mm^3, the mice were divided into six groups (n = 6): PBS with/without laser irradiation, ICG with/without laser irradiation, and aICG with/without laser irradiation. One hundred microliters of PBS, ICG, or aICG, in which ICG concentration was 13 µM, was injected locally to the tumor area. At 15 min after injection, the mice of laser irradiated group received 808 nm laser irradiation at 810 J/cm^2 for 15 min on the tumor area. The temperature change of the tumor area during the irradiation was recorded by the thermal camera at 0, 3, 5, 10, and 15 min. The short diameter (W) and long diameter (L) of the tumor was measured by an electrical caliper on day 0, 4, 7, 11, and 13. The volume of tumor (V) was calculated by the following equation: V = L × W^2 × 1/2. Bioluminescence derived from 4T-luc in the mice was measured using an *in vivo* imaging system (IVIS spectrum, PerkinElmer, USA) on day 13. On day 13, blood samples were corrected from the heart of the mice by syringes to measure AST, ALT, BUN, and CRE in the serum samples. The liver, kidney, and spleen of mice were harvested. The tissues were then fixed in 10% formalin at pH 7.4, and tissue cross-sections were histologically stained by hematoxylin and eosin (H & E) staining, followed by scanning using a digital slide scanner (NanoZoomer S210, Hamamatsu Photonics, Hamamatsu, Japan).

Statistical analysis

Statistical analyses between more than three groups and between two groups were conducted using one-way ANOVA followed by Tukey's test and using Student's t-test, respectively (Kaleida Graph 4.5 J; Synergy Software, Reading, PA, USA). A $p < 0.05$, was considered significant for all statistical analyses.

Results

Intercellular localization of aICG and ICG

In this study, we developed a copolymer of poly[2-(methacryloyloxy)ethyl]trimethylammonium chloride and poly[*N*-(3-aminopropyl)methacrylamide hydrochloride] conjugated with indocyanine green [PMETAC-*co*-PAPMAA(ICG)], referred to as aICG, in which indocyanine green is conjugated with a polycation bearing quaternary ammonium salt groups (Figure 1a). An average molecular weight of polycation bearing quaternary ammonium salt groups was approximately 20 kDa, it is positively charged and has high solubility in water. To investigate the impact of the polycation bearing quaternary ammonium salt groups, negatively charged ICG with molecular weight of 774.96 Da was used as a control (Figure 1b). As determined by measurement of absorption spectra of aICG and ICG in methanol by a UV-2600 UV-visible spectrophotometer (Shimadzu Corp., Kyoto, Japan), ICG concentration was 1.3 µM in both solutions (Figure 1c).

To observe intercellular distribution of aICG and ICG, in this study, 4T1 cells were stained by LysoTracker Green and Hoechst33258, which can be stained in lysosomes and nucleus, respectively. The fluorescence of ICG was detected in the cytoplasm (Figure 2a, b). On the region of interest (ROI) in a merged image of ICG- and Lysotracker-fluorescence images, most fluorescence signals of ICG were not overlapped with these of Lysotracker (Figure 2b to 2d). In contrast, the fluorescence signals of aICG were observed as dots in the cells (Figure 2a and c). On the ROI in enlarged merged image of ICG- and Lysotracker-fluorescence images, most fluorescence signals of ICG were overlapped with these of Lysotracker (Figure 2e to 2g). The ratio of cellular uptake was 17.6% for ICG, and 21.4% for aICG (Figure 2h).

Cell viability assay after laser irradiation

Anti-cancer activity of aICG upon the laser irradiation was evaluated using WST-1 assay. PBS, ICG (0.65 and 1.3 µM),

Fujiwara S., J Surg Res 2024
DOI:10.26502/jsr.10020350

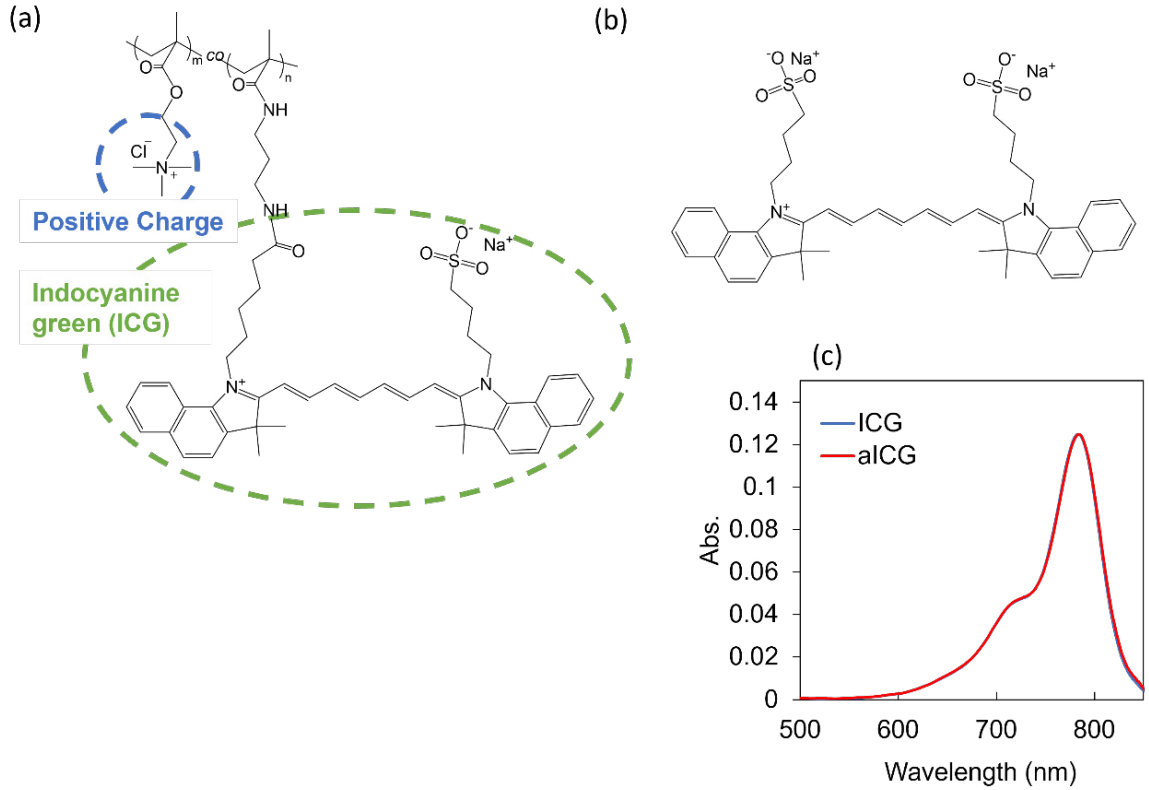

Figure 1: Chemical structures of (a) aICG and (b) ICG. (c) UV-vis absorption spectra of ICG and aICG in methanol. Indocyanine green concentration was 1.3 μM.

or aICG (0.65 and 1.3 μM) was added into the cell culture, followed by laser irradiation. First, temperature change of the culture medium was measured upon the laser irradiation at 0.9 W/cm^2 for 15 min (810 J/cm^2); there is no significant difference in the medium temperature between groups (Figure 3a). The cells survived in the any non-irradiated group and 0.65 μM ICG irradiated groups, while the 1.3 μM ICG irradiated group showed slightly anti-cancer efficacy. In contreast,the aICG irradiation group showed higher anti-cancer activity, compared to ICG (Figure 3b). Anti-cancer activity of aICG was also evaluated using LIVE/DEAD staining. The highest number of dead cells was observed in the 1.3 μM aICG irradiated group (Figure 3c).

Intracellular ROS generation

ROS generation was evaluated using DCFH-DA. DCFH-DA is deacetylated by intracellular esterases to non-fluorescent 2', 7'-dichlorodihydrofluorescin (DCFH). It is quickly oxidized by ROS to the highly fluorescent 2', 7'-dichlorodihydrofluorescein (DCF). The DCF was measured using flow cytometry. The fluorescence intensity in the non-irradiated group was similar for PBS, ICG, and aICG (Figure 4a, c). In the irradiated group, fluorescence intensity showed the higher increase in the aICG group upon the irradiation (Figure 4b, c).

Apoptosis/Necrosis assayApoptosis/Necrosis ssay

We used the Apoptosis/Necrosis Assay Kit including Apopxin Green Indicator (green), 7-AAD (red), and CytoCalcein Violet 450 (blue), to determine whether aICG-induced cell death is apoptosis or necrosis. In the aICG irradiated group, exposure of phosphatidylserine to the cell surface occurred immediately after irradiation, inducing apoptosis (Figure 5).

In vivo anti cancer NIR PTT by local administered aICG

The tumor temperature at the start of irradiation was approximately 34°C. During irradiation, the temperature of PBS, ICG, and aICG rose to a maximum of 37°C, 41°C, and 44°C, respectively. The temperatures of ICG and aICG reached their maximum at 5 min after the start of irradiation (Figure 6b). The effect of aICG on tumors was evaluated by comparing groups that received local injections of PBS, ICG, and aICG. No significant differences were shown in the non-irradiated group (Figure 6c). In the irradiated group, aICG significantly suppressed tumor growth as measured by calipers (Figure 6d). The similar results were obtained by measuring bioluminescence signals in the tumor with *In vivo* imaging system (IVIS Lumina III, PerkinElmer, USA) (Figure 6e, f).

Fujiwara S., J Surg Res 2024
DOI:10.26502/jsr.10020350

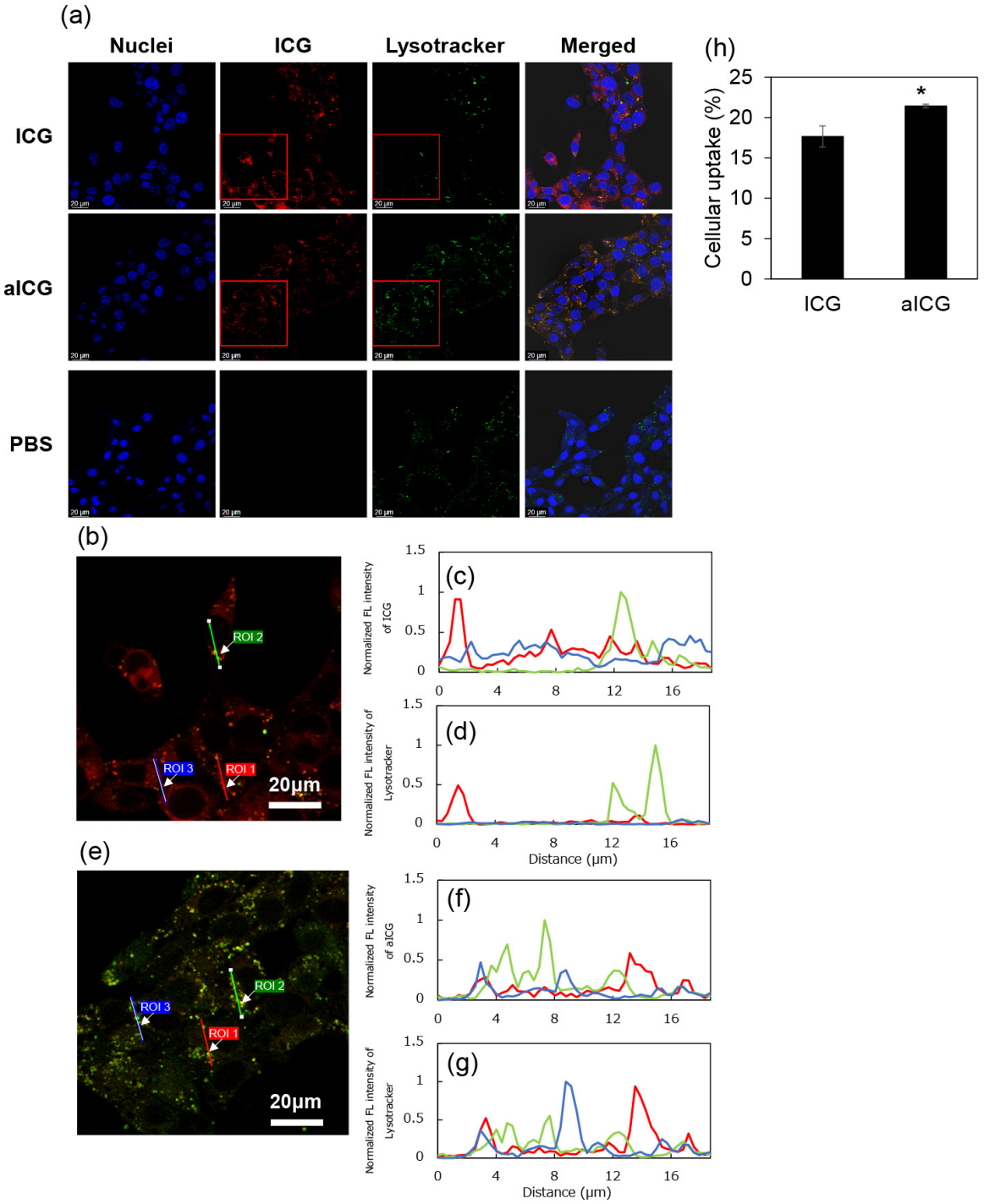

Figure 2: Intracellular uptake of ICG and aICG. (a) Image using laser scanning confocal microscopy of 4T1 cells incubated with ICG or aICG for 24 h. Nuclei were stained with DAPI (blue). Lysosome was stained with LysoTracker Green (green). ICG fluorescence are shown in red. Scale bars: 20 μm. **(b)** Enlarged merged image of ICG- and Lysotracker-fluorescences, which are shown as red square in figure 2a, with the region of interest (ROI) 1 to 3 **(c)** Normalized fluorescence intensity of ICG on the ROI 1 to 3 in the merged image of figure 2b **(d)** Normalized fluorescence intensity of Lysotracker on the ROI 1 to 3 in the merged image of figure 2b **(e)** Enlarged merged image of aICG- and Lysotracker-fluorescences with the ROI 1 to 3 **(f)** Normalized fluorescence intensity of aICG on the ROI 1 to 3 in the merged image of figure 2e **(g)** Normalized fluorescence intensity of Lysotracker on the ROI 1 to 3 in the merged image of figure 2e (**h**) Intracellular uptake of ICG after treatment with ICG or aICG. After cells were exposed to culture medium containing 1.3 μM of ICG for 24 h, the fluorescence intensity of ICG in the cell lysate was measured by fluorescence spectroscopy (Jasco, FP8500, Tokyo, Japan). Data are presented as means ± SD (n = 4). * $p < 0.005$.

Citation: Saori Fujiwara, Toru Yoshitomi, Aoi Hoshi, Van Thi Hong Doan, Yoshiki Komatsu, Huajian Chen, Naoki Kawazoe, Guoping Chen, Azusa Terasaki, Hiroko Bando, Hisato Hara, and Hirofumi Matsui. Locally administered photothermal therapy for breast cancer using endolysosome-targeted indocyanine green conjugated with polycation. Journal of Surgery and Research. 7 (2024): 122-133.

Fujiwara S., J Surg Res 2024
DOI:10.26502/jsr.10020350

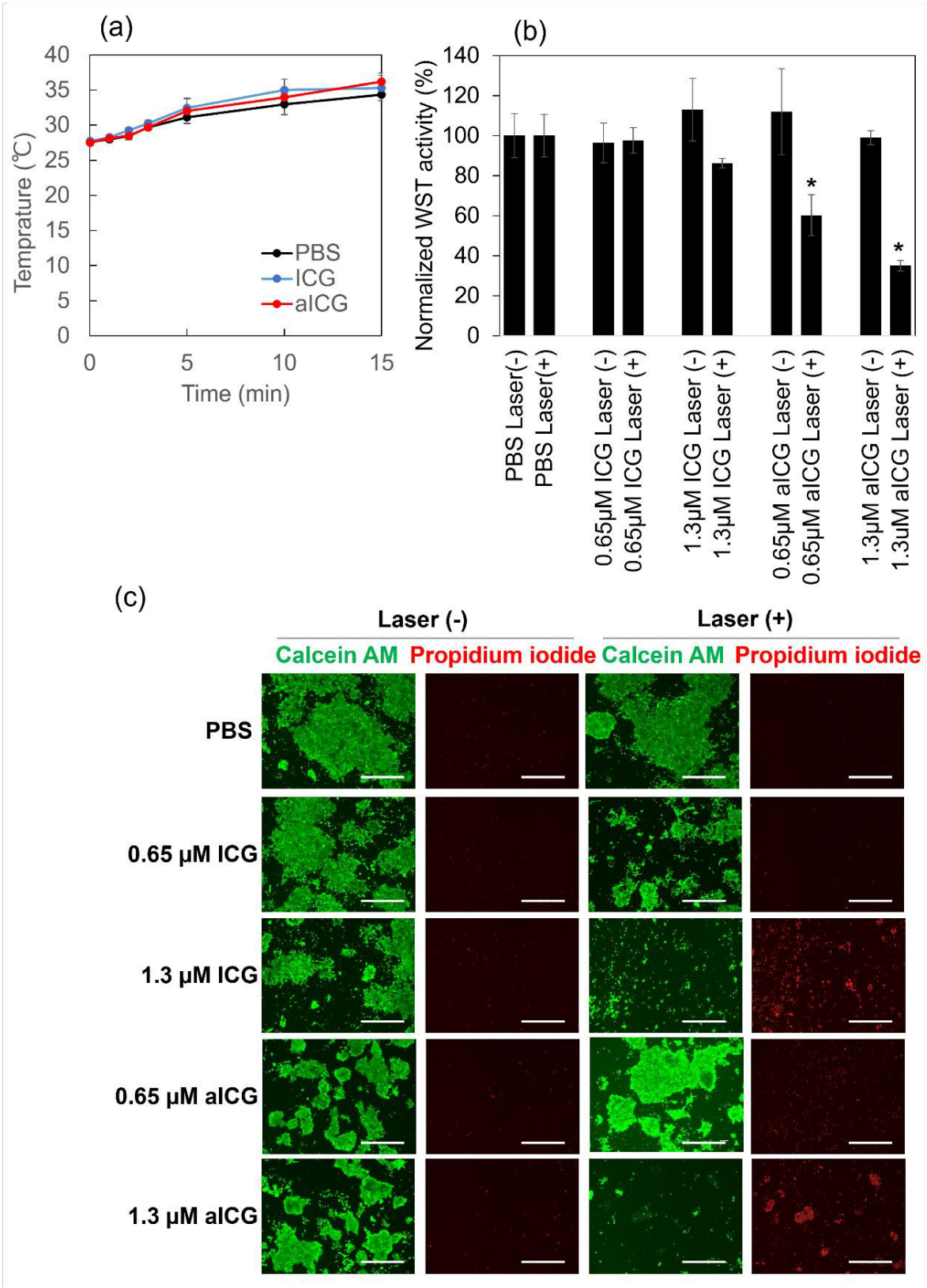

Figure 3: Anti-cancer activity of ICG and aICG. (**a**) Temperature change of culture medium upon laser irradiation at 0.9 W/cm^2 for 15 min (810 J/cm^2) (**b**) Cytotoxicity profile of ICG and aICG against 4T1 cells with and without laser irradiation. Irradiation was performed with 808 nm light at a density of 810 J cm^{-2}. Data represent means of normalized WST-1 activity with standard error (SEM) ($n = 3$; * $p < 0.05$). (**c**) LIVE/DEAD cell staining. Cells were treated with ICG and aICG at concentrations of 0.65 and 1.3 μM. Scale bars: 100 μm.

Citation: Saori Fujiwara, Toru Yoshitomi, Aoi Hoshi, Van Thi Hong Doan, Yoshiki Komatsu, Huajian Chen, Naoki Kawazoe, Guoping Chen, Azusa Terasaki, Hiroko Bando, Hisato Hara, and Hirofumi Matsui. Locally administered photothermal therapy for breast cancer using endolysosome-targeted indocyanine green conjugated with polycation. Journal of Surgery and Research. 7 (2024): 122-133.

Fujiwara S., J Surg Res 2024
DOI:10.26502/jsr.10020350

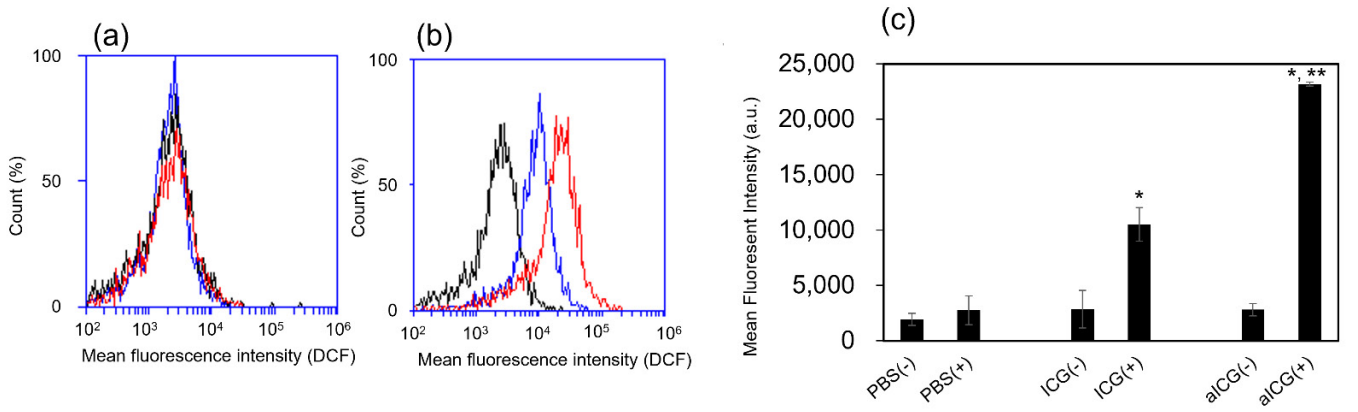

Figure 4: ROS generation in ICG/aICG-treated 4T1 cells, which detected with DCFH-DA. (**a**) Flow cytometry histogram of cells in the non-irradiated group. Blue: cells stained 24 h after addition of 1.3 μM ICG; black: cells stained as a control; red: cells stained 24 h after addition of 1.3 μM aICG. (**b**) Flow cytometry histogram of the cells in the irradiated group. Blue: cells stained 24 h after addition of 1.3 μM ICG; black: cells stained as a control; red: cells stained 24 h after addition of 1.3 μM aICG. (**c**) Median fluorescence intensity of 4T1 cells treated with PBS, ICG, and aICG with and without laser irradiation, in arbitrary units (a.u.). Data are shown as mean ± SEM ($n = 4$). * $p < 0.05$, compared with that without laser irradiation. ** $p < 0.05$, compared with PBS/ICG-treated group with laser irradiation.

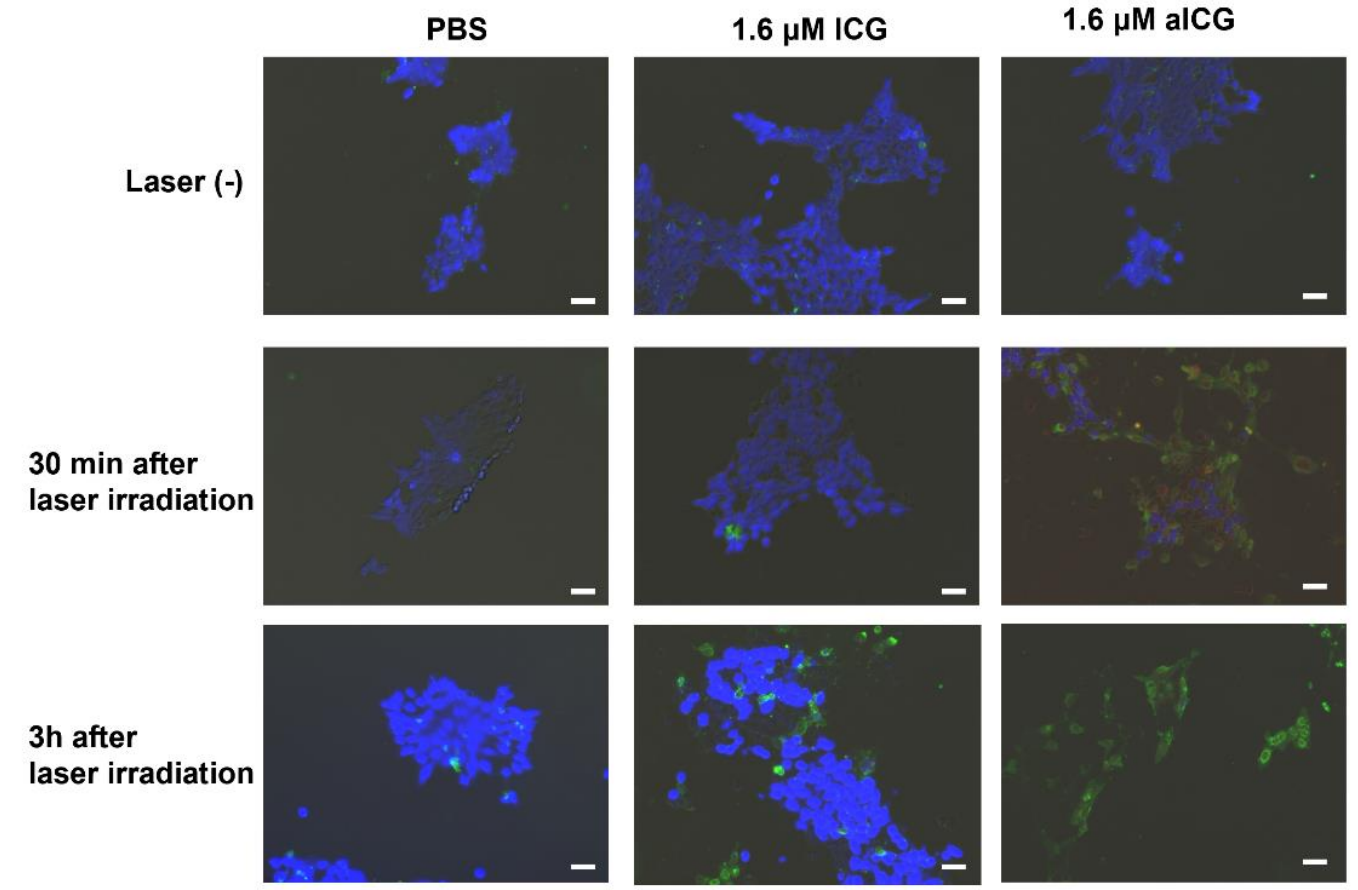

Figure 5: Microscopic observation with blue signals for live cells, green signals for early apoptotic cells, and red signals for late apoptotic/necrotic cells. Cells were stained using an Apoptosis/Necrosis Assay kit at 30 min or 3 h after laser irradiation. Scale bars: 20 μm. The Apoptosis/Necrosis Assay kit consists of three dyes: CytoCalcein Violet 450 (blue) for viable cells, Apopxin Green Indicator (green) for early apoptotic cells, and 7-AAD (red) for late apoptotic/necrotic cells.

Citation: Saori Fujiwara, Toru Yoshitomi, Aoi Hoshi, Van Thi Hong Doan, Yoshiki Komatsu, Huajian Chen, Naoki Kawazoe, Guoping Chen, Azusa Terasaki, Hiroko Bando, Hisato Hara, and Hirofumi Matsui. Locally administered photothermal therapy for breast cancer using endolysosome-targeted indocyanine green conjugated with polycation. Journal of Surgery and Research. 7 (2024): 122-133.

Fujiwara S., J Surg Res 2024
DOI:10.26502/jsr.10020350

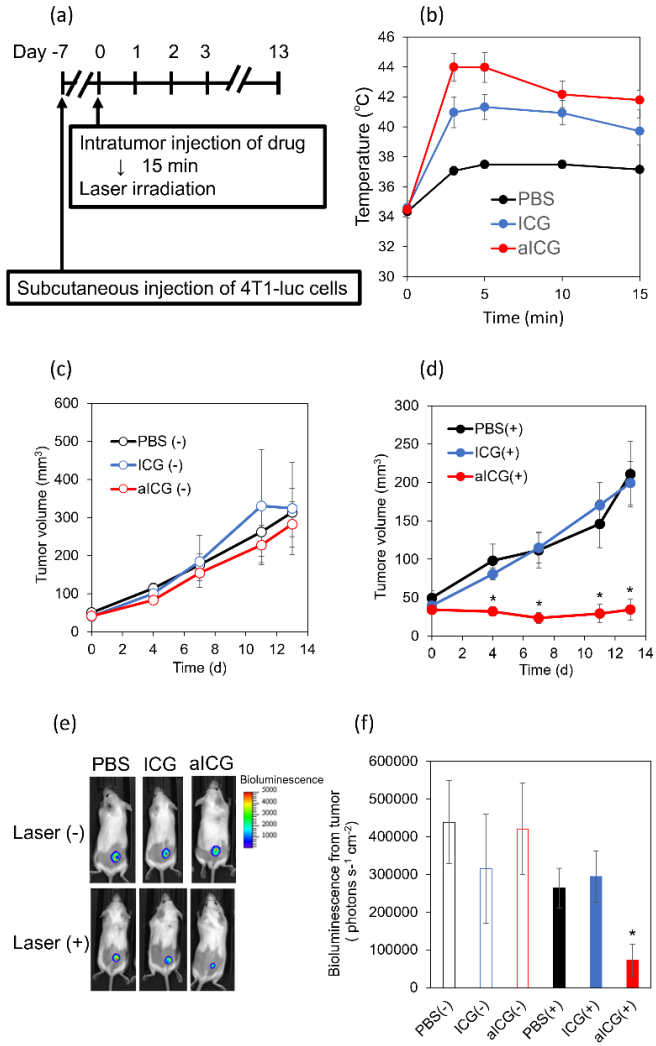

Figure 6: ***In vivo*** **antitumor effect of aICG.** (**a**) Experimental schedule (b) Temperature change in the tumor sites upon the laser irradiation. Data are shown as mean ± SEM (n = 6). (**c, d**) Tumor volume change in the group (c) without and (d) with 808 nm laser irradiation at 810 J cm^{-2}. Data are shown as mean ± SEM (n = 6). * $p < 0.05$, as compared to PBS/ICG-treated mice. (e) Representative *in vivo* images of bioluminescence from cancer cells in PBS-, ICG-, and aICG-treated mice with and without laser irradiation on day 13. The rainbow images show the relative intensities of bioluminescence ranging from low (dark blue), to medium (light blue/green), to high (yellow/red). (**f**) Bioluminescence intensity of 4T1-luc cells in the tumor. ** $p < 0.05$, compared with ICG-treated group with laser irradiation.

Safety of locally administered aICG

To examine adverse events caused by local administration of aICG to the tumor area, body weight measurements, the H&E staining of the organ, and blood tests were conducted. As shown in figure 7a, no group of mice showed weight loss. H&E stained images showed no obvious abnormal findings in the liver, kidney, and spleen (Figure 7b). Blood tests showed no significantly abnormal findings in the aICG-treated groups (Table 1). All groups had mild elevations in AST and ALT, but there were no obvious abnormal findings in the liver specimens obtained at autopsy, and the findings in the blood tests suggest that some hemolysis may have occurred during blood collection. Based on these results, the safety concern associated with local administration of aICG is considered to be low.

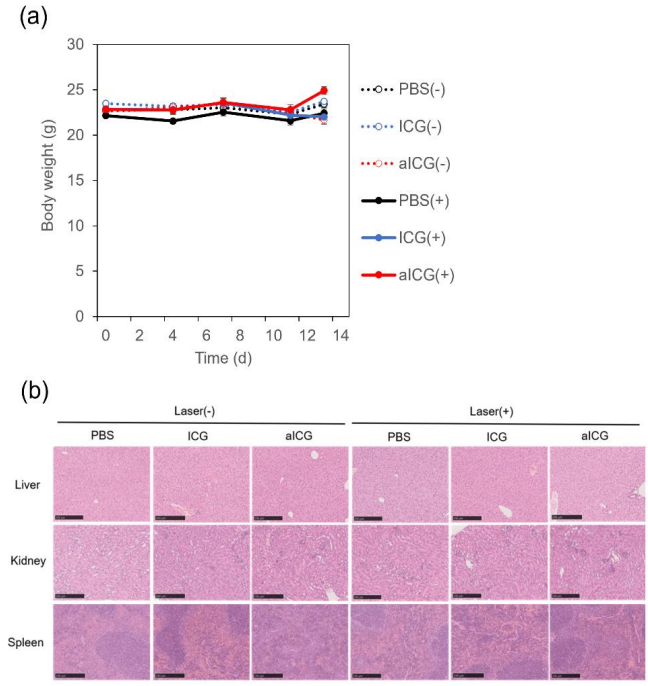

Figure 7: (a) Body weight of mice in different groups after treatment, closed circles represent the data for irradiation, open circles for no irradiation, and (b) H&E stained images of the liver, kidney, and spleen on day 13. Scale bars: 250 μm.

Table 1: Serum levels of AST, ALT, CRE and BUN

	Laser (-)			Laser (+)		
	PBS	ICG	aICG	PBS	ICG	aICG
AST (U/dL)	366 ± 109	247 ± 41	215 ± 48	146 ± 28	207 ± 43	164 ± 34
ALT (U/dL)	151 ± 15	74 ± 14	140 ± 46	73 ± 12	62 ± 5	86 ± 15
CRE (mg/dL)	0.12 ± 0.02	0.14 ± 0.04	0.17 ± 0.04	0.14 ± 0.03	0.10 ± 0.02	0.13 ± 0.02
BUN (mg/dL)	27 ± 1	22 ± 1	22 ± 2	24 ± 2	24 ± 1	24 ± 2

Citation: Saori Fujiwara, Toru Yoshitomi, Aoi Hoshi, Van Thi Hong Doan, Yoshiki Komatsu, Huajian Chen, Naoki Kawazoe, Guoping Chen, Azusa Terasaki, Hiroko Bando, Hisato Hara, and Hirofumi Matsui. Locally administered photothermal therapy for breast cancer using endolysosome-targeted indocyanine green conjugated with polycation. Journal of Surgery and Research. 7 (2024): 122-133.

Fujiwara S., J Surg Res 2024
DOI:10.26502/jsr.10020350

Discussion

Endolysosomes are generated by the fusion of late endosome and lysosome, and decompose endogenous and exogenous biomolecules such as carbohydrates, lipids, nucleic acids, and peptides [17,18]. When the membrane of endolysosome is damaged, the contents including digestive enzymes within the endolysosome leak out, causing apoptosis [13-15]. As endocytosis has been reported to be more prevalent in cancer cells than that in normal cells [19], endolysosomal membrane would be an attractive target for cancer therapy.

The intracellular distribution of drugs has a major impact on the therapeutic efficacy. The structural features of a drug including its charge, molecular weight, and balance of hydrophilicity/hydorophobicity influences the intracellular distribution. ICG is a hydrophobic compound with a divalent negative charge, and its molecular weight is 774.96 Da. As shown in figure 2, ICG can penetrate cell membranes, enters the cytoplasm, and is confined in the hydrophobic pockets of proteins. On the other hand, the intracellular distribution of aICG is influenced by the feature of polycation, because ICG is bound to a hydrophilic polycation with a molecular weight of approximately 20 kDa. Indeed, as shown in figure 2, the intracellular distribution of aICG was significantly different from that of low-molecular-weight ICG, and completely overlapped with the Lysotracker fluorescence signal. LysoTracker probes consist of a hydrophobic fluorescent compound with a weak base, and can diffuse in the cells. At an acidic environment within the lysosome including endolysosome, the weakly basic moiety is protonated. The protonated probe can not diffuse across the organelle membrane, providing an accumulation in the lysosomes including endolysosome. Polycations in aICG electrostatically adhere to negatively charged polysaccharides on cell membranes and are then uptaken into cells by endocytosis. After the aICG-incorporated endosome is fused with the lysosome, aICG would reach the endolysosome. The interaction of aICG and ICG with the cell membrane would also be different. The lysosome-associated membrane proteins are highly glycosylated and negatively charged [17,20]. As the low-molecular-weight ICG has a negative charge, it would electrostatically repel the polysaccharide. On the other hand, aICG has a positive charge and would adhere to polysaccharide on the endolysosomal membranes. As a result, aICG would increase membrane permeability of endolysosomes by the NIR photohermal effect. In recent years, antibody- and peptide-drugs have attracted attention. However, as they are degraded by digestive enzymes within the endolysosome, they cannot be used for endolysosomal targeted PTT. Although the detailed mechanism still needs to be analyzed, this study shows the higher anti-cancer effect of endolysosome-targeted NIR-PTT with aICG in the *in vitro* experiments.

Breast cancer is a tumor close to the body surface and the drugs can be easily punctured under echo-guided injection [21,22]. ICG and aICG were locally injected into the tumor of breast cancer model in mice. Upon the NIR light irradiation, at the ICG- and aICG-injected sites, the intratumoral temperature rose to a temperature range called therapeutic hyperthermia, which is defined as the local heating of a tumor to 40–44 °C [23]. Normal tissues are rarely affected by temperatures below 45 °C [23]. Both aICG and ICG increased the intratumoral temperature to the temperature range of therapeutic hyperthermia, yet aICG was higher anti-tumor effect than ICG in the tumor-bearing mice. Probably, this is because ICG rapidly diffused within the tissue. An important point is that the temperature within the tumor was kept within 45 °C. Thermal therapy above 50 °C causes burns and becomes painful. Therefore, locally administered PTT using aICG would be a painless and non-invasive treatment. As described in introduction, for patients with locally advanced breast cancer and/or with advanced age or underlying diseases, the development of a painless and noninvasive local treatment that can reduce the tumor size effectively is desired as another options besides chemotherapy. As NIR-PTT with aICG can be reliably injected into the tumor sites of breast cancer under echo-guidance, and reduce tumor size by NIR irradiation without any adverse effects, it has the potential as a next-generation preoperative therapy in the field of breast cancer treatment. Drug therapy for breast cancer includes hormonal therapy, anticancer drugs, and antibody therapy. For example, hormone therapy is effective for estrogen receptor-positive breast cancer, and anti-HER2 drugs such as trastuzumab and pertuzumab have been shown to be effective for HER2-positive breast cancer in which HER2 protein is overexpressed in cancer cells [24]. However, patients with triple-negative breast cancer do not benefit from hormone therapy or anti-HER2 drugs due to a lack of related receptors. As endocytosis occurs in all cancer cells regardless of subtype, locally-administered NIR-PTT with aICG might be effective in triple-negative breast cancer.

Conclusions

In this study, we demonstrate that aICG has a higher anti-tumor effect *via* the apoptosis pathway due to the endolysosome targeting property of aICG. To our knowledge, there is no report about development of endolysosome-targeted ICG derivatives. In addition, we confirmed that NIR-PTT with intratumor injection of aICG shows a higher anti-tumor effect upon the light irradiation at 808 nm, compared to low-molecular-weight ICG. Taken together, the strategies of endolysosome-targeted PTT must improve the efficacy of phototherapy dramatically. Thus, aICG has the potential to be the next-generation photothermal agent for locally administered NIR-PTT.

Citation: Saori Fujiwara, Toru Yoshitomi, Aoi Hoshi, Van Thi Hong Doan, Yoshiki Komatsu, Huajian Chen, Naoki Kawazoe, Guoping Chen, Azusa Terasaki, Hiroko Bando, Hisato Hara, and Hirofumi Matsui. Locally administered photothermal therapy for breast cancer using endolysosome-targeted indocyanine green conjugated with polycation. Journal of Surgery and Research. 7 (2024): 122-133.

Fujiwara S., J Surg Res 2024
DOI:10.26502/jsr.10020350

Disclosure statement

No potential conflict of interest was reported by the author(s).

Author Contributions

Conceptualization, T.Y., S.F., A.H., A.T. and H.M.; methodology, S.F., H.C. and T.Y.; validation, S.F. and T.Y.; formal analysis, S.F. and T.Y.; investigation, S.F., Y.K., V.D., and T.Y.; resources, T.Y., N.K., and G.C.; data curation, S.F. and T.Y.; writing—original draft preparation, S.F. and T.Y.; writing—review and editing, all coauthors; visualization, S.F. and T.Y.; supervision, T.Y. and H.M; project administration, T.Y. and H.M; funding acquisition, T.Y., N.K., G.C. and H.M. All authors have read and agreed to the published version of the manuscript.

Acknowledgements

This study was partially supported by the Japan Society for the Promotion of Science KAKENHI under Grant [number 21H03813 (to T.Y., G.C., N.K., and H.M.) and 22K15574 (A.T.)].

References

1. Kocarnik JM, Compton K, Dean FE, et al. Cancer Incidence, Mortality, Years of Life Lost, Years Lived With Disability, and Disability-Adjusted Life Years for 29 Cancer Groups From 2010 to 2019: A Systematic Analysis for the Global Burden of Disease Study 2019: JAMA Oncol 8 (2022): 420-444.
2. Anderson BO, Ilbawi AM, Fidarova E, et al.The Global Breast Cancer Initiative: a strategic collaboration to strengthen health care for non-communicable diseases:Lancet Oncol 22 (2021): 578-581.
3. G. Early Breast Cancer Trialists' Collaborative.Long-term outcomes for neoadjuvant versus adjuvant chemotherapy in early breast cancer: meta-analysis of individual patient data from ten randomised trials:Lancet Oncol 19 (2018): 27-39.
4. Sutrisno L, Chen H, Yoshitomi T, et al. PLGA-collagen-BPNS Bifunctional composite mesh for photothermal therapy of melanoma and skin tissue engineering: J Mater Chem B 10 (2022): 204-213.
5. Sutrisno L, Chen H, Chen Y, et al. Composite scaffolds of black phosphorus nanosheets and gelatin with controlled pore structures for photothermal cancer therapy and adipose tissue engineering: Biomaterials 275 (2021): 120923.
6. Sun J, Zhao H, Xu W, et al. Recent advances in photothermal therapy-based multifunctional nanoplatforms for breast cancer: Front Chem 10 (2022):1024177.
7. S.G. Alamdari, M. Amini, N. Jalilzadeh, et al.Recent advances in nanoparticle-based photothermal therapy for breast cancer: J Control Release 349 (2022): 269-303.
8. X. Li, J.F. Lovell, J. Yoon, et al. Clinical development and potential of photothermal and photodynamic therapies for cancer: Nat Rev Clin Oncol 17 (2020): 657-674.
9. Polom K, Murawa D, Rho YS, et al. Current trends and emerging future of indocyanine green usage in surgery and oncology: a literature review: Cancer 117 (2011): 4812-4822.
10. Faybik P, Hetz H.. Plasma disappearance rate of indocyanine green in liver dysfunction: Transplant Proc 38 (2006): 801-812.
11. Miranda D, Wan C, Kilian HI, et al. Lovell, Indocyanine green binds to DOTAP liposomes for enhanced optical properties and tumor photoablation:Biomater Sci 7 (2019): 3158-3164.
12. Ballabio A. The awesome lysosome:EMBO Mol Med 8 (2016): 73-76.
13. Johansson AC, Appelqvist HC, Nilsson, et al. Regulation of apoptosis-associated lysosomal membrane permeabilization:Apoptosis 15 (2010): 527-540.
14. Boya P, Kroemer G. Lysosomal membrane permeabilization in cell death, Oncogene 27 (2008): 6434-6451.
15. Wang F, Gomez-Sintes R, Boya P. Lysosomal membrane permeabilization and cell death: Traffic 19 (2018): 918-931.
16. Komatsu Y, Yoshitomi T, Doan VTH, et al. Locally Administered Photodynamic Therapy for Cancer Using Nano-Adhesive Photosensitizer: Pharmaceutics 15 (2023): 20-76.
17. Winchester BG. Lysosomal membrane proteins: Eur J Paediatr Neurol 5 Suppl A (2001): 11-19.
18. Huotari J, Helenius A. Endosome maturation: EMBO J 30 (2011): 3481-3500.
19. Mellman I, Yarden Y. Endocytosis and cancer:Cold Spring Harb Perspect Biol 5 (2013): 016949.
20. Thelen AM, Zoncu R. Emerging Roles for the Lysosome in Lipid Metabolism:Trends Cell Biol 27 (2017): 833-850.
21. Kooistra B, Wauters C, Strobbe L, et al. Preoperative cytological and histological diagnosis of breast lesions: A critical review. Eur J Surg Oncol 36 (2010):934-940.
22. Bhatt AA, Whaley DH, Lee CU. Ultrasound-Guided Breast Biopsies: Basic and New Techniques: J Ultrasound Med 40 (2021): 1427-1443.

Fujiwara S., J Surg Res 2024
DOI:10.26502/jsr.10020350

23. Kwon S, Jung S, Baek SH. Combination Therapy of Radiation and Hyperthermia, Focusing on the Synergistic Anti-Cancer Effects and Research Trends:Antioxidants (Basel) 12 (2023): 924.

24. Loibl S, Poortmans P, Morrow M, et al. Breast cancer:Lancet 397 (2021): 1750-1769.

Citation: Saori Fujiwara, Toru Yoshitomi, Aoi Hoshi, Van Thi Hong Doan, Yoshiki Komatsu, Huajian Chen, Naoki Kawazoe, Guoping Chen, Azusa Terasaki, Hiroko Bando, Hisato Hara, and Hirofumi Matsui. Locally administered photothermal therapy for breast cancer using endolysosome-targeted indocyanine green conjugated with polycation. Journal of Surgery and Research. 7 (2024): 122-133.

Fujiwara S., J Surg Res 2024
DOI:10.26502/jsr.10020350

SUPPLEMENTARY FILES

S1. Chemicals

Indocyanine green NHS ester (ICG-NHS) was purchased from BioActs (Incheon, Korea). Trypsin-EDTA, [2-(methacryloyloxy)ethyl]trimethylammonium chloride (METAC), and *N*-(3-aminopropyl)methacrylamide hydrochloride (APMAA) were purchased from Sigma-Aldrich (St Louis, Missouri, USA). Methanol, RPMI-1640 medium with L-glutamine and phenol red, and *N*-hydroxysuccinimide (NHS) were purchased from FUJIFILM Wako Pure Chemical (Osaka, Japan). Fetal bovine serum was purchased from Gibco (Waltham, MA, USA). RIPA buffer was purchased from Nacalai Tesque (Kyoto, Japan). 1-Ethyl-3-(3-dimethylaminopropyl)-carbodiimide hydrochloride (WSCD-HCl) was purchased from Peptide Institute, Inc. (Osaka, Japan). The LIVE/DEAD Cell Staining Kit was purchased from Dojindo (Kumamoto, Japan). The Apoptosis/Necrosis Assay Kit (Catalog No.: ab176749) was purchased from Abcam (Cambridge, UK). RPMI 1640 medium without phenol red was purchased from Thermo Fisher Scientific (San Jose, CA, USA). 2',7'-Dichlorodihydrofluorescein diacetate was purchased from Santa Cruz Biotechnology (Santa Cruz, Santacruz, CA).

S2. Preparation of PMETAC-*co*-PAPMAA(ICG)

poly[2-(methacryloyloxy)ethyl]trimethylammonium chloride and poly[*N*-(3-aminopropyl)methacrylamide hydrochloride] (PMETAC-*co*-PAPMAA) was synthesized according to previous report [1]. The weight- and number-average molecular weights of the obtained polymer, PMETAC-*co*-PAPMAA, were 54,500 and 23,500, respectively, and its polydispersity index (PDI) was 2.32, as determined by size exclusion chromatography [1]. The average unit numbers of PMETAC and PAPMAA in PMETAC-*co*-PAPMAA were 200 and 2, respectively [1]. PMETAC-*co*-PAPMAA (80 mg), 2 mL of phosphate buffer solution (pH 7.0) containing ICG-NHS (6.2 mg), WSCD-HCl (31.0 mg), and NHS (23.0 mg) were was added into a 10-mL flask, and stirred for 20 h at 25 °C. To purify PMETAC-*co*-PAPMAA(ICG), using a pre-swollen membrane tube (Spectra/Por; molecular-weight cutoff size: 3500), dialysis was conducted for 24 h against 2 L of water, followed by freeze-drying. The yield of the obtained polymer was 84.8% (73.0 mg). PMETAC-*co*-PAPMAA(ICG) is called adhesive indocyanine green (aICG). UV–vis spectra of aICG were measured by a UV-2600 UV-visible spectrophotometer (Shimadzu Corp., Kyoto, Japan). aICG was dissolved in PBS at a concentration of 2.5 mg/mL, in which the concentration of indocyanine green was 13 μM. As determined by the measurement of absorbance at 760 nm, one ICG molecule was introduced into a molecule of PMETAC-*co*-PAPMAA.